INL/CON-23-71507-Revision-0

Multi-scale modeling of the electric field assisted sintering process

March 2023

Changing the World's Energy Future

Larry Kenneth Aagesen Jr, Stephanie A Pitts, Lucas Robinson, R. Edwin Garcia

Idaho National Laboratory

INL/CON-23-71507-Revision-0

Multi-scale modeling of the electric field assisted sintering process

Larry Kenneth Aagesen Jr, Stephanie A Pitts, Lucas Robinson, R. Edwin Garcia

March 2023

Idaho National Laboratory
Idaho Falls, Idaho 83415

http://www.inl.gov

Prepared for the
U.S. Department of Energy
Under DOE Idaho Operations Office
Contract DE-AC07-05ID14517

Multi-scale modeling of the electric field assisted sintering process

Larry Aagesen, Stephanie Pitts
Idaho National Laboratory
Lucas Robinson, R. Edwin Garcia
Purdue University

Idaho National Laboratory

Introduction: Electric-Field Assisted Sintering (EFAS)

- Technique for powder consolidation using simultaneous application of heat, pressure, electric field
- Allows consolidation of powders (metal, ceramic) with lower energy input compared with hot pressing
- Potential applications relevant to Idaho National Lab (INL)'s mission:
  - Nuclear fuel pellets, moderator and reflector materials, heat exchangers, hydrogen production
- INL is investing in experimental and modeling & simulation capabilities to study EFAS. Test case: Y_2O_3
  - Modeling microstructural evolution: Phase-field

DCS-800

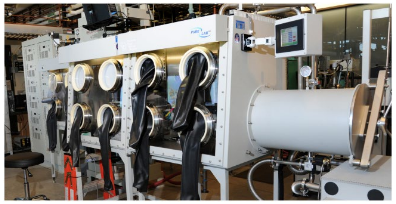

Rad EFAS

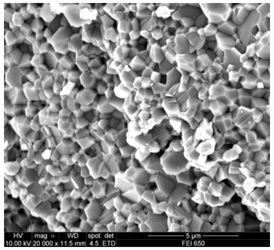

EFAS Y_2O_3

MALAMUTE: Mod-sim of Advanced Manufacturing

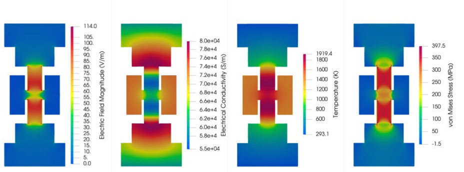

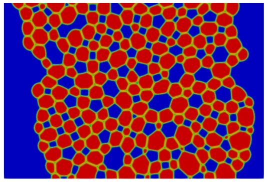

Microstructure in the Phase-field Model

Grain 1:
$\eta_1 = 1, \eta_2 = 0, \phi = 0$

Grain 2:
$\eta_1 = 0, \eta_2 = 1, \phi = 0$

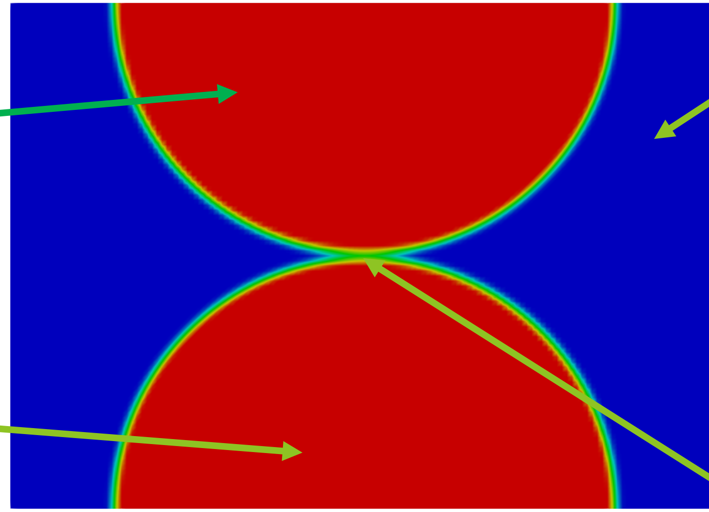

Void:
$\eta_1 = 0, \eta_2 = 0, \phi = 1$

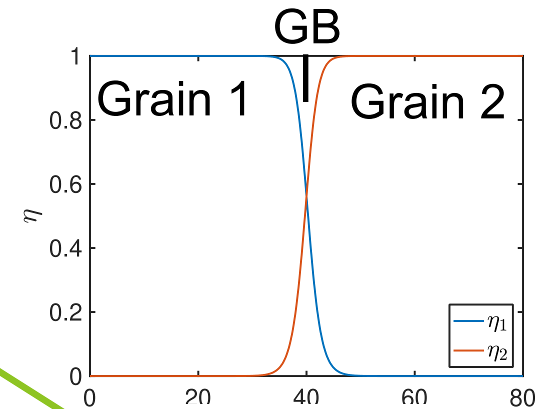

Diffuse interface

- Order parameters $\eta_1, \eta_2, \ldots$ represent grains of the solid Y_2O_3
- Order parameter ϕ represents the void phase
  - Diffuse interface between order parameters represents grain boundaries (GBs), surfaces
- Vacancy species V_Y''' and $V_O^{\circ\circ}$, corresponding densities n_{V_Y} and n_{V_O}
  - Void phase composed entirely of vacancies with $n_{V_Y} = n_Y$ and $n_{V_o} = n_o$

Phase-Field Model: Grand-Potential Functional

$$\Omega = \int_V \left(m \left[\sum_\alpha \sum_{i=1}^{p_\alpha} \left(\frac{\eta_{\alpha i}^4}{4} - \frac{\eta_{\alpha i}^2}{2} \right) + \sum_\alpha \sum_{i=1}^{p_\alpha} \left(\sum_\beta \sum_{j=1, \alpha i \neq \beta j}^{p_\beta} \frac{\gamma_{\alpha i \beta j}}{2} \eta_{\alpha i}^2 \eta_{\beta j}^2 \right) + \frac{1}{4} \right] + \frac{\kappa}{2} \sum_\alpha \sum_{i=1}^{p_\alpha} |\nabla \eta_{\alpha i}|^2 + \sum_\alpha h_\alpha \omega_\alpha \right) dV$$

- Multi-phase, multi-order parameter extension to grand-potential model[2]
- Advantages:
  - Bulk free energy contribution is removed from interfacial energy
  - Allows interfacial thickness and energy to be set independently, enabling coarser mesh, improved computational performance
  - Similar to KKS in this respect, but do not need separate phase concentration variables, so performance is improved
  - Prevents spurious formation of additional phases at two-phase interfaces

[2] L.K. Aagesen, Y. Gao, D. Schwen, K. Ahmed, *Phys. Rev. E*, 98, 023309 (2018).
L.K. Aagesen, D. Schwen, M.R. Tonks, Y. Zhang, *Comp. Mat. Sci.*, 161, 35-45 (2019).

Electrochemical grand potential densities

- Typically, phase-field models use Helmholtz free energy
  - Solid and void phases: $f_{ec,s}$ and $f_{ec,v}$
- To take advantage of grand potential formulation, need to perform Legendre transform of each phase's Helmholtz free energy to obtain electrochemical grand potential densities of solid and void phases, ω_s and ω_v:

$$\omega_s = f_{ec,s} - \mu_{V_Y} n^s_{V_Y} - \mu_{V_O} n^s_{V_O} - \vec{D} \cdot \vec{E}$$

$$\omega_v = f_{ec,v} - \mu_{V_Y} n^v_{V_Y} - \mu_{V_O} n^v_{V_O} - \vec{D} \cdot \vec{E}$$

- μ_{V_Y}, μ_{V_o} : chemical potentials
- Transforms independent variables to μ_{V_Y}, μ_{V_o}, V

Electrochemical free energies of each phase

- Sum of chemical and electrostatic energy contributions: for solid,

$$f_{ec,s} = f_{chem,s} + f_{es,s}$$

- Chemical contribution: dilute solution or parabolic approximation

$$f^{d}_{chem,s} = n^{s}_{V_Y} E^{s}_{V_Y} + n_Y kT \left(c^{s}_{V_Y} \ln c^{s}_{V_Y} - c^{s}_{V_Y} \right) + n^{s}_{V_O} E^{s}_{V_O} + n_O kT \left(c^{s}_{V_O} \ln c^{s}_{V_O} - c^{s}_{V_O} \right)$$

- To account for vacancy segregation energy to GBs,

$$E^{s}_{V_Y} = \left(E^{f}_{V_Y} + A \left(E^{GB}_{V_Y} - E^{f}_{V_Y} \right) (1-\lambda)^2 \right) \qquad \lambda = \sum_{i=1}^{n} \eta_i^2$$

- Electrostatic contribution:

$$f_{es,s} = \rho V + \frac{1}{2} \vec{D} \cdot \vec{E} \qquad \rho = \sum_i Z_i e n_i \qquad \vec{D} = \epsilon_s \vec{E}$$

Evolution Equations

- Allen-Cahn Equations for Order parameters:

$$\frac{\partial \eta_i}{\partial t} = -L_s \frac{\delta \Omega}{\delta \eta_i} \qquad \frac{\partial \phi}{\partial t} = -L_v \frac{\delta \Omega}{\delta \phi}$$

- Vacancy concentration evolution: Chemical Potential

$$\chi_{V_Y} \frac{\partial \mu_{V_Y}}{\partial t} = \nabla \cdot \chi_{V_Y} \mathbf{D}_{V_Y} \nabla \mu_{V_Y} - \left(\frac{\partial n_{V_Y}}{\partial \phi} \frac{\partial \phi}{\partial t} + \sum_i \frac{\partial n_{V_Y}}{\partial \eta_i} \frac{\partial \eta_i}{\partial t} \right)$$

- Vacancy diffusivities higher at GBs (10^6), surfaces (10^9)
- Electric potential: split into equilibrium potential V and homogeneous solution δV (deviation due to applied E-field)

$$\frac{\delta \Omega}{\delta V} = 0 \qquad \frac{\partial \rho}{\partial t} = \nabla \cdot s \nabla \delta v \approx 0 \qquad s = \sum_i \frac{e^2 Z_i^2 n_i D_i}{kT}$$

- Joule heating:

$$\dot{q} = s \left| \nabla \delta V \right|^2$$

Phase-field implementation: MOOSE

- MOOSE (Multi-physics Object-Oriented Simulation Environment): general purpose PDE solver based on finite element framework
  - Adaptive meshing, implicit time stepping, GrainTracker
- Open source and free via mooseframework.inl.gov

MOOSE

Phase Field | Tensor Mechanics | Heat Conduction

MARMOT

Phase-field & microstructure-dependent properties for nuclear materials

MALAMUTE: Advanced Manufacturing

No physics

Applicable to all materials Free!

MOOSE-Based Applications (need license)

Defect segregation to Grain Boundaries: 1D

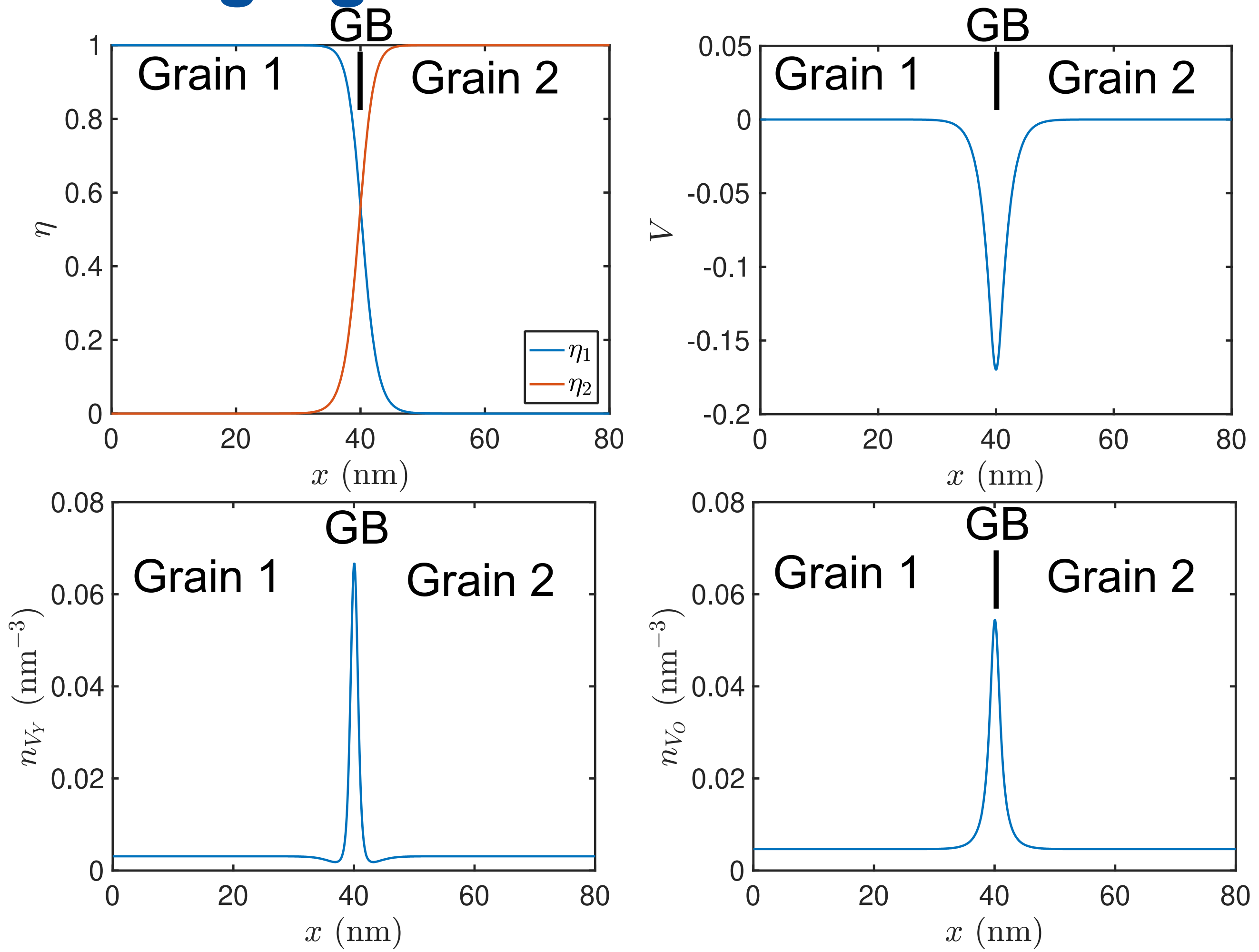

- Lower formation energies at GBs gives elevated vacancy concentrations, charge imbalance
  - Results in electric potential difference

Microstructure evolution and neck growth of two-particle contact

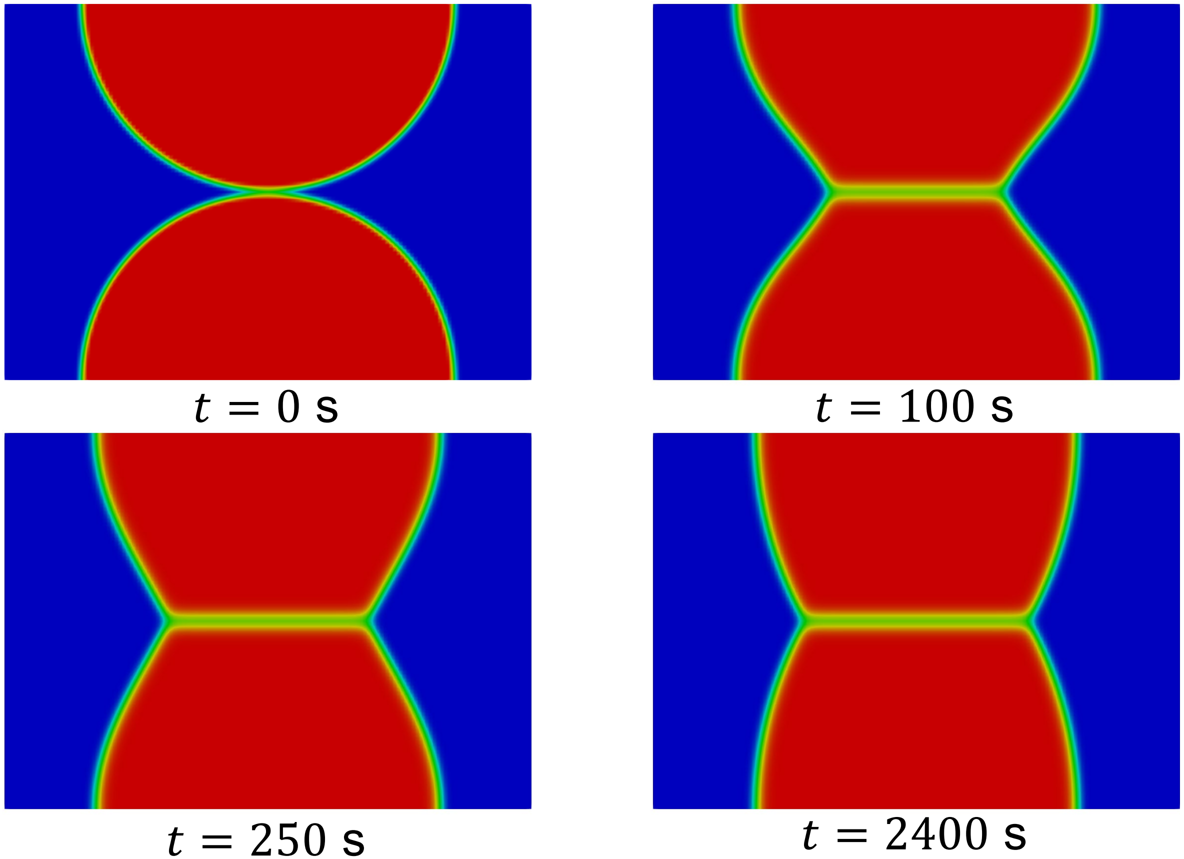

- Two particles in contact with initial particle radius
  - Varying initial radius R and applied E-field
  - Shown here: R = 50 nm and E = 4000 V/m

Enhanced electrical conductivity and heat generation along surfaces, GBs

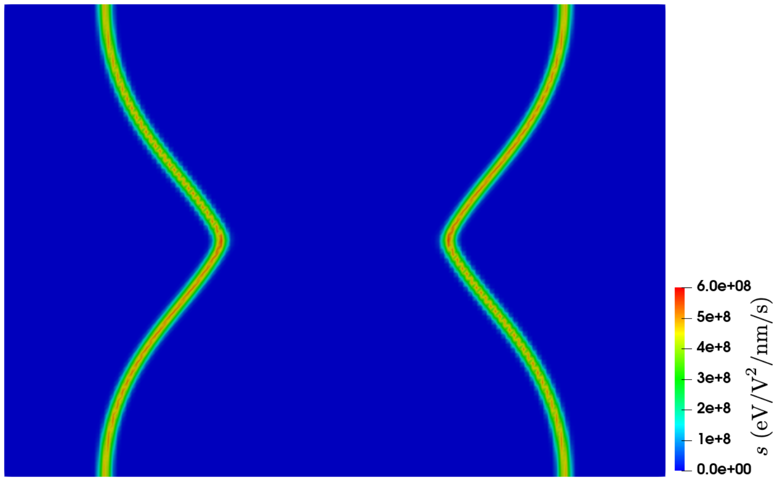

Electrical conductivity

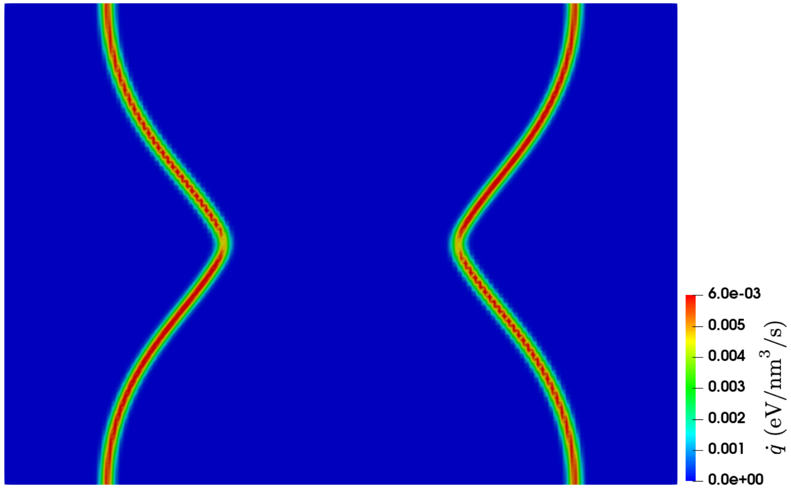

Heat generation

- Electrical conductivity enhanced at surfaces, grain boundaries due to enhanced defect diffusivity
- Local heat generation primarily located to surfaces in this geometry due to surface enhancement of diffusivity
- Heat redistributes very rapidly in particles compared to time scale of EFAS process
  - Assume local temperature rise can be found from volume-average of heat generation

Neck grows faster for smaller particles

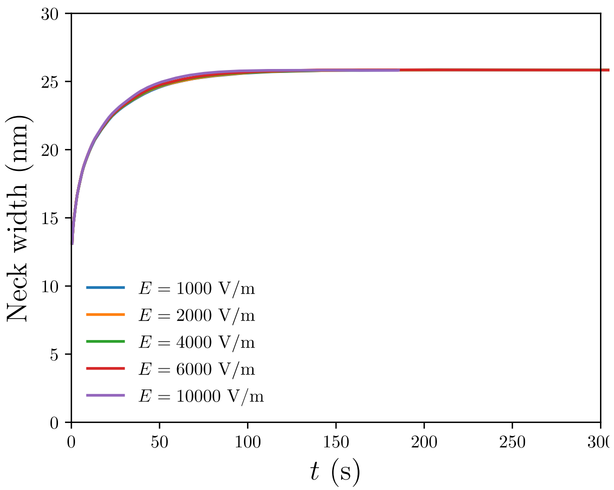

Initial $R = 20$ nm

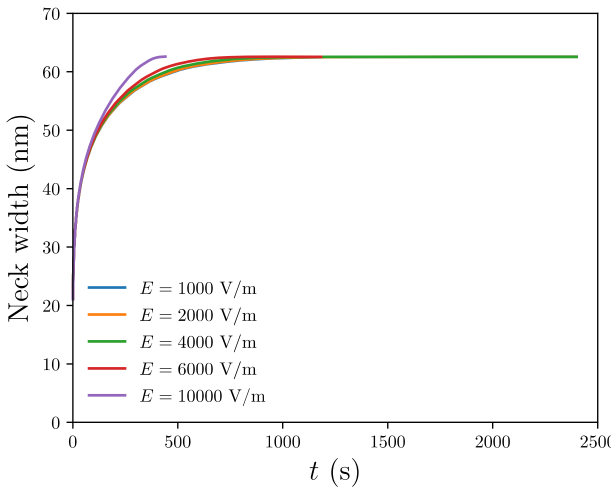

Initial $R = 50$ nm

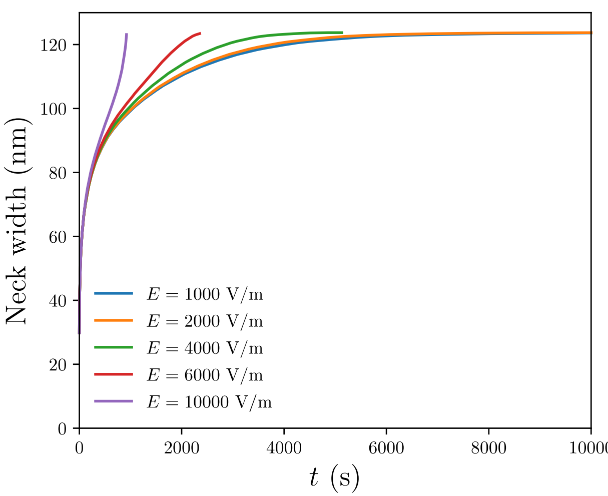

Initial $R = 100$ nm

- Increasing E-field causes acceleration of neck growth for larger particles

Temperature increase accelerates with increasing E-field

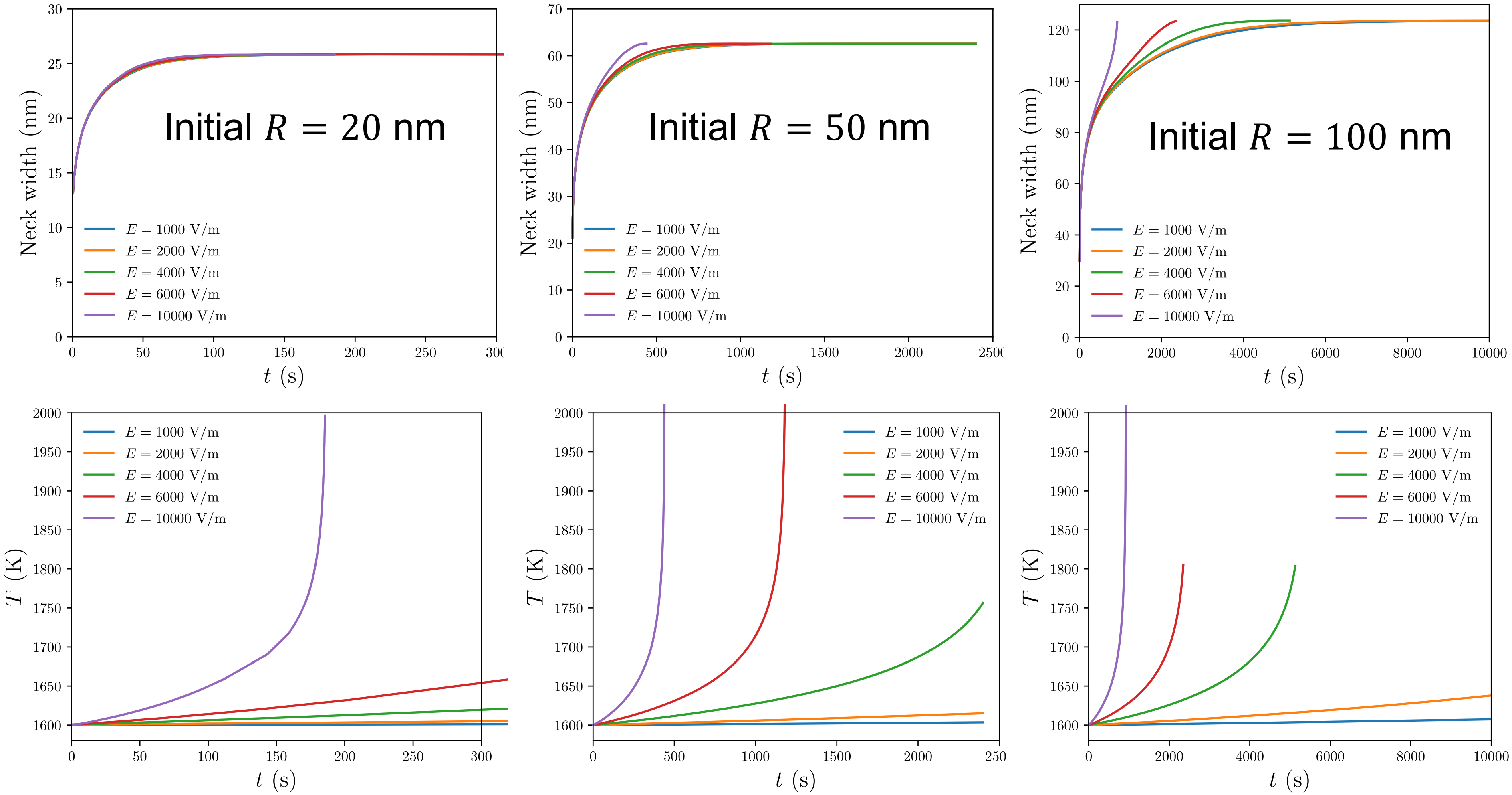

- E-field causes temperature spike sooner relative to neck growth for larger particles

Many-particle simulations

- Initial radius $R = 150$ nm, $E = 1000$ V/m

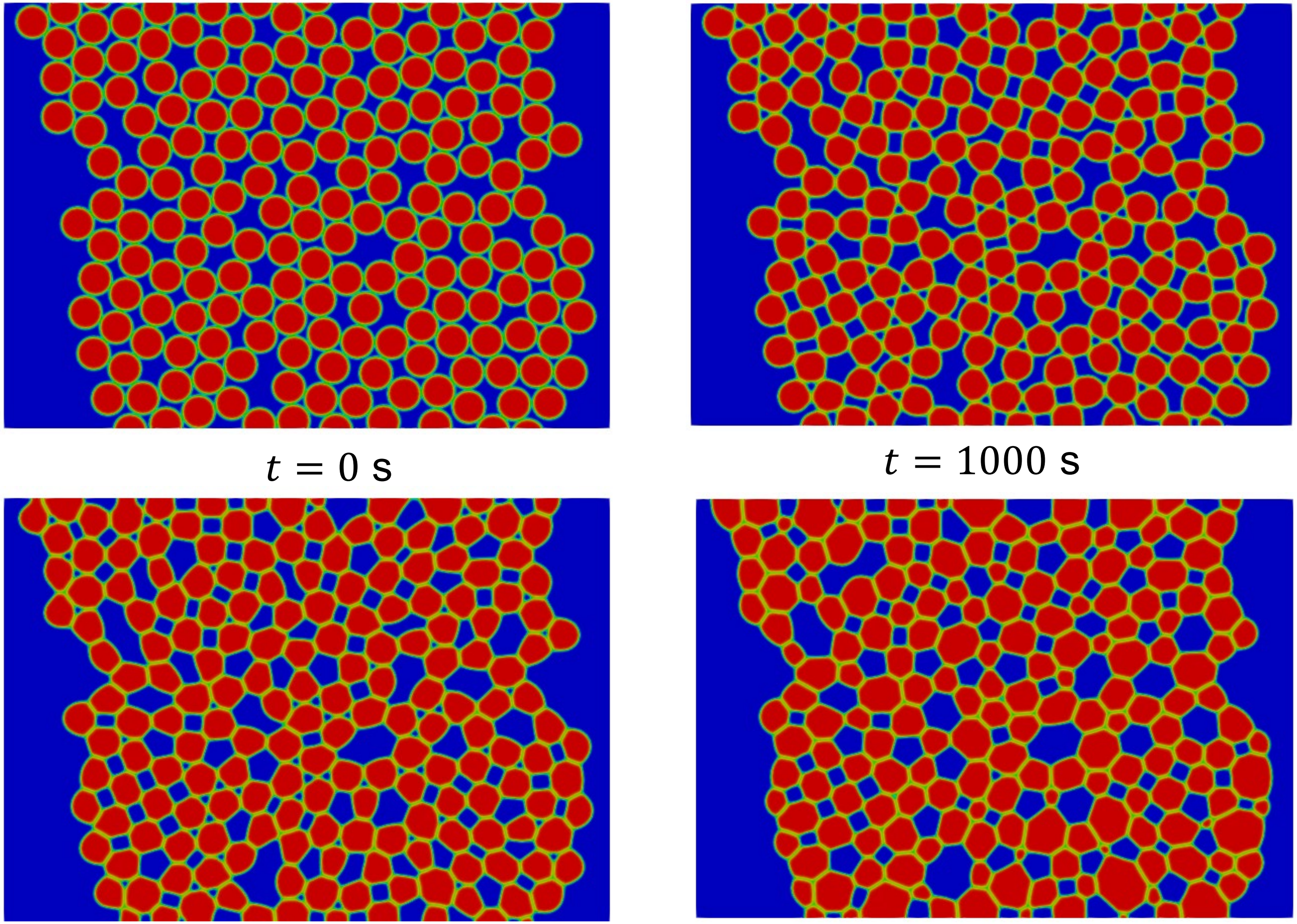

$t = 0$ s

$t = 1000$ s

$t = 10{,}000$ s

$t = 40{,}000$ s

Conductivity and heat generation

- Grain structure overlaid in black
- Enhanced conductivity on surfaces, GBs
  - Highest conductivity on internal, external surfaces
- Highest heat generation rate on external surfaces
- Many significant localized heat spots internally

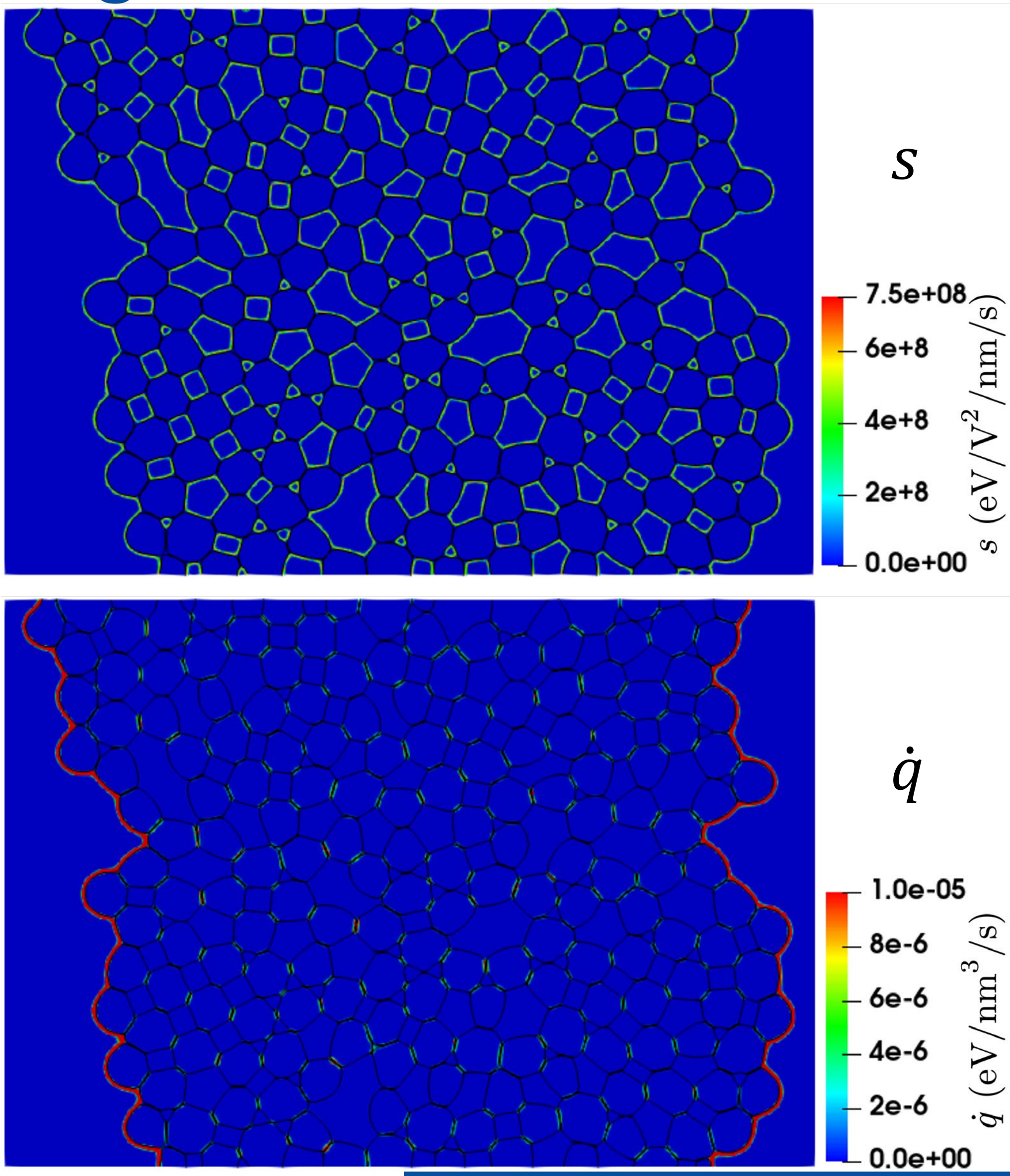

Internal heat generation

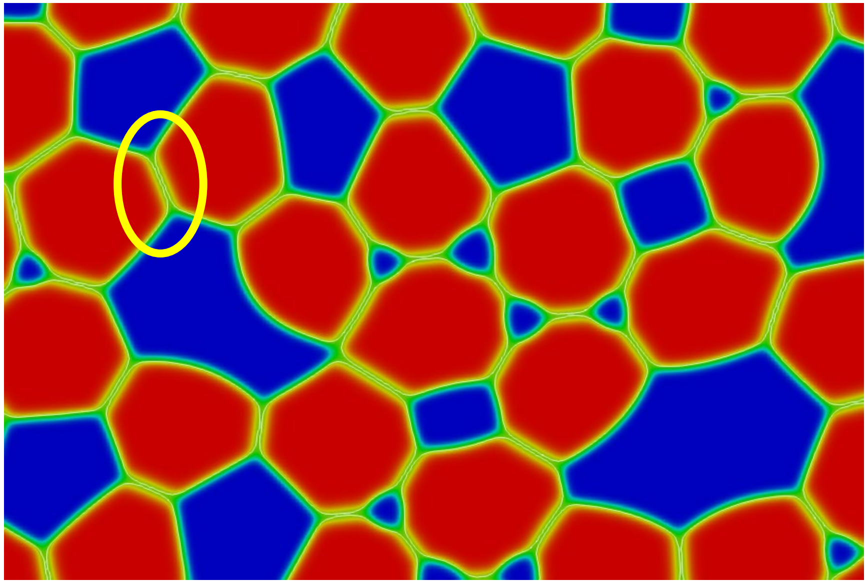

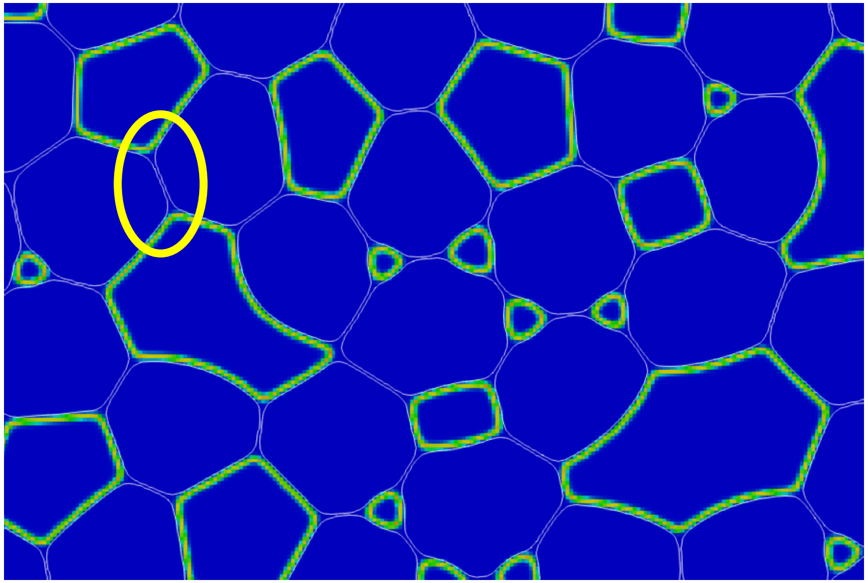

s

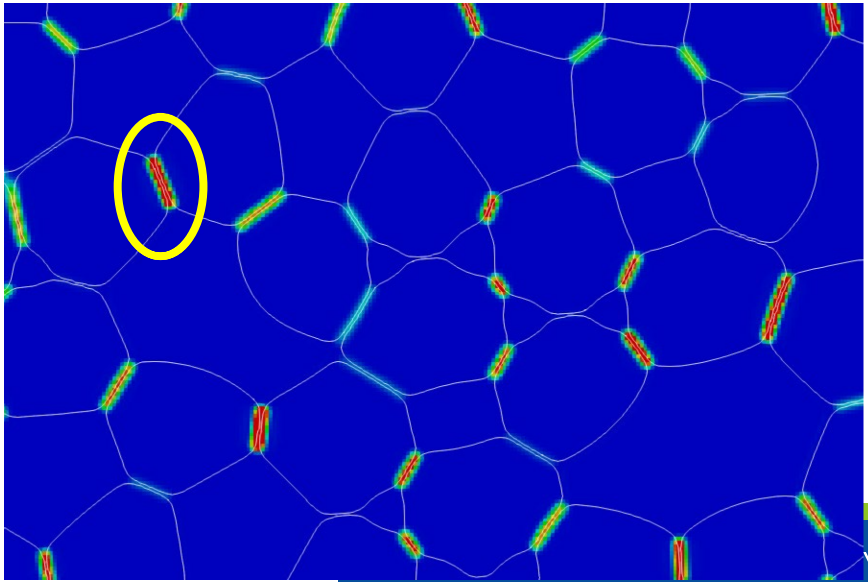

$\dot{q}$

- Although conductivity is much higher on internal surfaces than GBs, internally, heat generation is localized to GBs
- ?

Internal heat generation

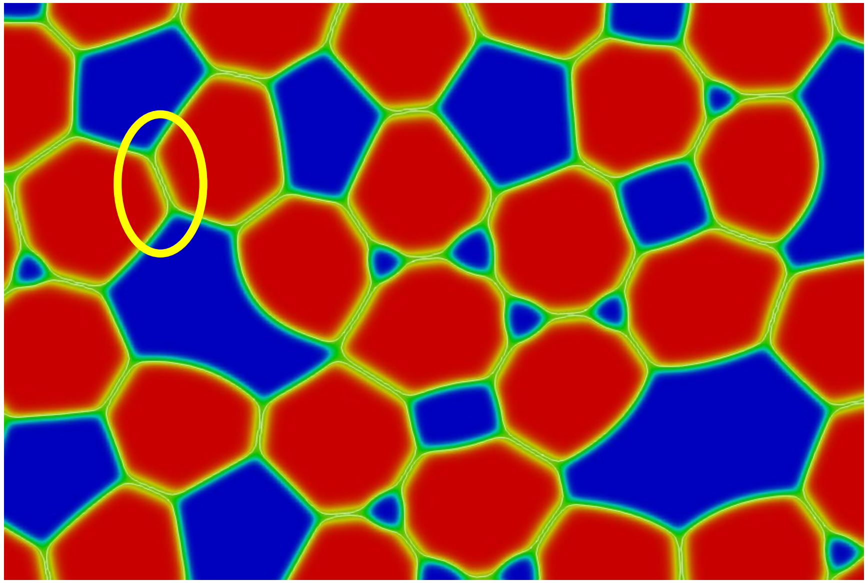

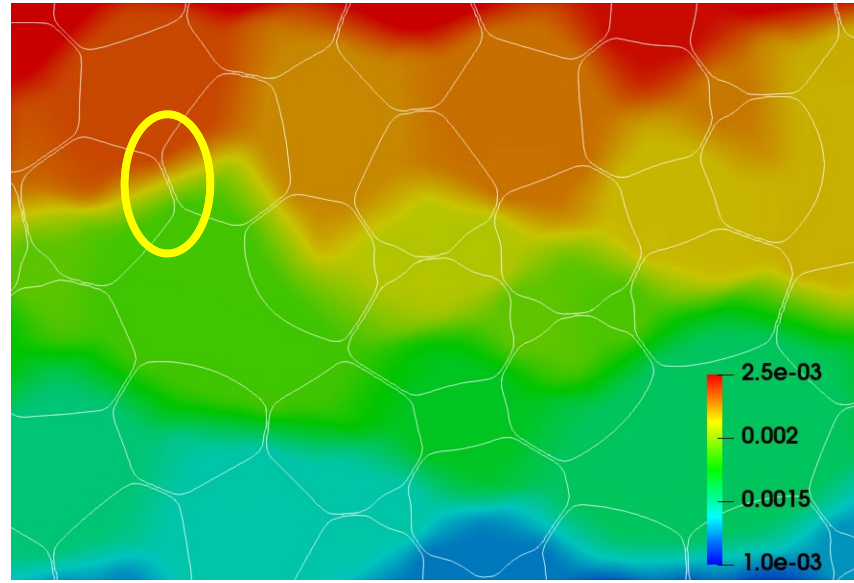

δV

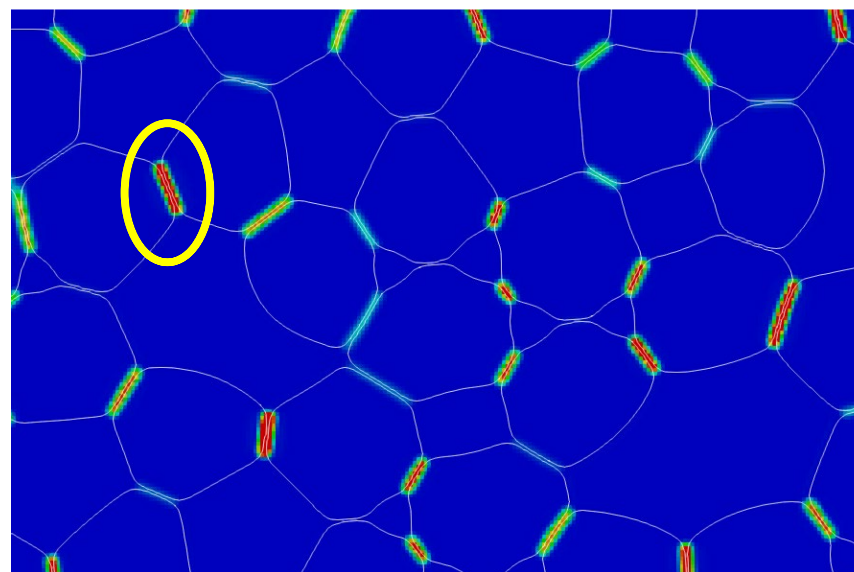

$\dot{q}$

- Applied potential δV drop localized to grain boundaries
- Since , drop in δV dominates
- In experiments, continuous surface pathway is less likely, so generation at GBs should dominate

Multi-scale simulation Framework

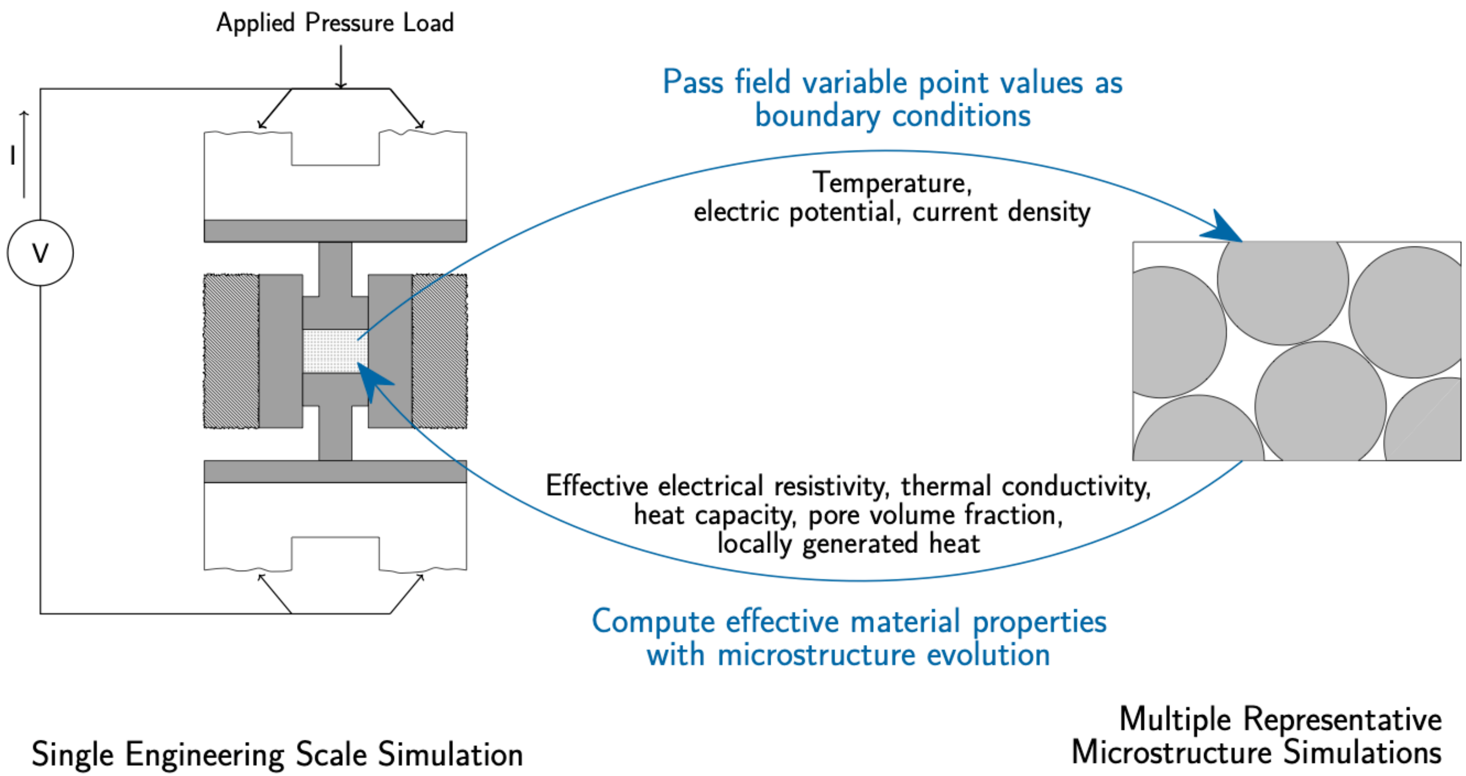

MALAMUTE

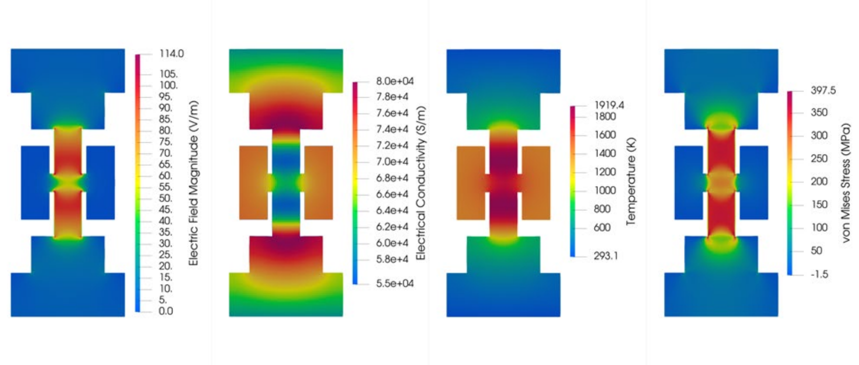

Conclusions

- Developed phase-field model of EFAS process that accounts for grain structure, defect species, electric field due to charged defects and applied electric field
  - Computationally efficient due to grand potential formulation
  - Extensible to other materials and arbitrary number of defect species
- Simulated neck growth rate in 2-particle configuration
  - Applied E-field has increasing impact for larger particles
- Simulated multi-particle configuration
  - Local heating localized to GBs
- Multi-scale framework linking engineering to meso-scale
- Future work:
  - Integrate plastic flow effects into electrochemical phase-field model, validate
  - Run multi-scale process simulations, validate

Thank you!

Funding Support: INL LDRD Program

Questions?

Idaho National Laboratory